

A study of corneal structure and biomechanical properties after collagen crosslinking with genipin in rabbit corneas

Yun Tang, Wenjing Song, Jing Qiao, Bei Rong, Yuan Wu, Xiaoming Yan

Department of Ophthalmology, Peking University First Hospital

Purpose: Aim to assess the short-term effect of genipin collagen crosslinking (G-CXL) on corneal structure and biomechanical properties compared with ultraviolet A/riboflavin collagen crosslinking (UVA-CXL) in rabbit corneas.

Methods: Right eyes of 40 healthy rabbits were divided into the 0.20% G-CXL group, 0.25% G-CXL group, UVA-CXL group, and control group. Anterior segment optical coherence tomography (ASOCT) and in vivo confocal microscopy (IVCM) were performed before, 7 days after, and 14 days after the CXL treatment. Corneal strips were harvested for tensile strain measurements 7 and 14 days after the CXL treatment.

Results: ASOCT showed the demarcation line (DL) in the UVA-CXL group was deeper than in the 0.20% G-CXL group and the 0.25% G-CXL group on day 7 ($p=0.014$) and day 14 ($p=0.012$). Nerve and keratocyte density in all CXL groups decreased, but was more obvious in the UVA-CXL group ($p<0.001$). Endothelial cell loss in the 0.20% G-CXL group, 0.25% G-CXL group, UVA-CXL group, and control group was 11.7%, 6.8%, 32.8%, and 2.0% 14 days after CXL, respectively. Young's modulus and stress in the 0.25% G-CXL group and the UVA-CXL group were statistically significantly higher than in the control group ($p<0.05$) 7 and 14 days after CXL. No statistically significant differences were observed between the 0.25% G-CXL group and the UVA-CXL group ($p>0.05$). The DL depth was positively correlated with Young's modulus ($r=0.426$, $p=0.042$) and stress ($r=0.469$, $p=0.024$).

Conclusions: The administration of 0.25% genipin enhances corneal biomechanical properties as long as 14 days after the CXL treatment with low toxicity. The DL exists in CXL-treated corneas, and the depth is related to the biomechanical properties.

Corneal collagen crosslinking (CXL) is a new treatment for corneal ectasia and keratoconus. Ultraviolet A/riboflavin CXL (UVA-CXL) has been proved to be an effective procedure to strengthen the cornea, improve visual acuity, and halt the progression of keratoconus [1-4]. However, UVA leads to keratocyte apoptosis [5], changes in corneal sensitivity [6] and endothelial cell loss, especially in thin corneas [7,8]. Thus, new crosslinking agents with low cornea toxicity are needed.

Genipin is a natural CXL agent extracted from *Gardenia jasminoides*. Animal studies showed genipin can increase the stiffness of the cornea [9,10] and sclera [11], and the resistance of the cornea to enzymatic digest [12], with lower toxicity to endothelial cells compared to UVA-CXL [9]. Genipin crosslinked chitosan materials and hydrogel membranes have an excellent biocompatibility with eye tissues [13,14]. This evidence indicates genipin corneal collagen crosslinking (G-CXL) is an effective, low-cytotoxic, and promising new method for corneal collagen crosslinking.

Despite the positive results for G-CXL, thus far, most studies have been conducted on ex vivo animal models, and only instant effects were reported. Further in vivo studies on changes in the corneal structure and long- and short-term biomechanical properties of the cornea after the administration of G-CXL are needed. In this study, the effect of G-CXL on corneal structure and biomechanical properties was evaluated in a 14-day observation, compared with UVA-CXL.

METHODS

Animals: Healthy New Zealand albino rabbits (weight 3.0–3.5 kg) were selected, and no corneal abnormality was found with slit-lamp biomicroscopy before the experiments were conducted. All animal procedures adhered to the Chinese Ministry of Science and Technology Guidelines on the Humane Treatment of Laboratory Animals (Vgkfcz-2006–398) and the ARVO Statement for the Use of Animals in Ophthalmic and Vision Research. This study was approved by the animal ethics committee of Peking University First Hospital (no. 201454).

Right eyes of 40 rabbits were equally divided into the 0.20% G-CXL group, 0.25% G-CXL group, UVA-CXL group, and control group. Anterior segment optical coherence tomography (ASOCT) and in vivo confocal microscopy (IVCM) were performed before, 7 days after, and 14 days

Correspondence to: Xiaoming Yan, Department of Ophthalmology, Peking University First Hospital, No.8 Xishiku Avenue, Beijing, China; Phone: +86-10-83573953; FAX: +86-01086102748; email: yanxiaoming7908@163.com

after the CXL treatment. On day 7 and 14 after the CXL treatment, five rabbits in each group were euthanized with an intravenous overdose injection of 5% pentobarbital (1 mg/kg, Sinopharm Chemical Reagent Co., Ltd, Shanghai, China). Then the corneal strips were harvested for tensile strain measurements.

Surgical method: Genipin powder (Wako Pure Chemical Industry, Osaka, Japan) was dissolved in PBS buffer (1X, pH 7.3±0.2, ZSGB-BIO, Beijing, China) to a concentration of 0.20% or 0.25%. Rabbits were placed under general anesthesia of 5% pentobarbital (0.5 ml/kg, obtained from the Peking University First Hospital Animal Center) and ocular surface anesthesia of 0.4% oxybuprocaine hydrochloride (Benoxil, Santen Pharmaceutical Co. Ltd., Osaka, Japan).

For the G-CXL group, the central 8 mm of the corneal epithelium were removed for better penetration. Then a drop of 0.20% or 0.25% genipin solution was applied on the cornea every 2 min for 30 min. During the interval of genipin application, the eyelids were closed to avoid stroma dehydration. UVA-CXL was performed following the Dresden protocol [15]. After the CXL treatment in the G-CXL and UVA-CXL groups was completed, the extra CXL agent was washed away with sterile saline. In the control group, only corneal epithelial debridement was applied. For each group, Loxacin gel (Sinqi Pharmaceutical, Shenyang, China) was applied daily to prevent infection.

ASOCT and IVCN: All rabbits underwent ASOCT (Heidelberg Engineering, Heidelberg, Germany) and IVCN (HRT3 RCM, Heidelberg Engineering, Heidelberg, Germany) scans in vivo to evaluate changes in corneal morphology before and after CXL treatment. If a well-defined demarcation line (DL) was observed on the ASOCT images, the depth from the corneal surface to the DL at the center cornea was measured with the software on ASOCT. Five nonoverlapping images of the subepithelium nerve, cornea stroma, and endothelial cells were selected from IVCN for quantified analysis. The average cell count of keratocytes and endothelium cells was calculated with software on IVCN. NeuronJ, a semiautomated tracing plugin program for ImageJ, was used for nerve density analysis [16,17].

Tensile strain measurement: Seven or 14 days after the CXL treatment, five rabbits in each group were euthanized with an overdose of 5% pentobarbital (Sinopharm Chemical Reagent Co., Ltd, Shanghai, China). A 4-mm-wide vertical corneal strip was harvested from the central cornea at 12 o'clock with a double-bladed scalpel.

The tensile strain test was performed at a temperature of 23±2.0 °C and relative humidity of 50–60%. The corneal

strips were vertically clamped between jaws in a computer-controlled microtester (5848 MicroTester, Instron, Norwood, State). The distance between the jaws was 10 mm. Then the corneal strips were stretched at a speed of 2 mm/min until a maximum force of 5N was reached, or the tissue ruptured.

The stress-deformity curve was obtained from the microtester. Young's modulus and stress at 10% strain were calculated by fitting the curve with the exponential function .

Statistical analysis: SPSS 20.0 (IBM Corporation, Armonk, NY) was used for all statistical analyses. The mean ± standard deviation of Young's modulus, stress, DL depth, cornea nerve density, stroma keratocyte density, and endothelial cell count are presented. Outcome measures comparisons among groups at different time points were analyzed using one-way ANOVA. The stroma keratocyte density before and after the CXL treatment was compared with the Student *t* test. DL depth differences between 7 and 14 days after the CXL treatment were analyzed with the Student *t* test. The Pearson correlation coefficient was used to analyze the correlation of the biomechanical properties and the DL depth. Statistical significance was set at the $\alpha = 0.05$ level.

RESULTS

ASOCT and DL: A well-defined DL were visible in 9/10 eyes in the 0.20% G-CXL group and 8/10 eyes in the 0.25% G-CXL group on 7 and 14 days after the CXL treatment (Figure 1A,B, arrows). The deepest position of the DL was mainly located on the edge of the pupil (Figure 1A,B, arrowhead). A DL was visible in all ten eyes in the UVA-CXL group on 7 and 14 days after the CXL treatment (Figure 1C, arrows). The deepest position of the DL was located in the central cornea (Figure 1C, arrowhead). No DL in the control group was observed (Figure 1D).

Seven days after the CXL treatment, the DL depth in the 0.20% G-CXL group ($n = 5$), 0.25% G-CXL group ($n = 3$), and UVA-CXL group ($n = 5$) was 144.2±24.10, 206.3±80.40, and 241.6±24.70 μm , respectively ($p=0.014$). And 14 days after CXL treatment, the DL depth was shallower compared to day 7 ($p>0.05$). The DL depth in the 0.20% G-CXL group ($n = 4$), 0.25% G-CXL group ($n = 5$), and UVA-CXL group ($n = 5$) was 120.8±23.10, 182.4±65.50, and 233.0±31.70 μm , respectively ($p=0.012$). The DL in the UVA-CXL group was statistically significant deeper than in the 0.20% G-CXL group 7 days ($p=0.004$) and 14 days ($p=0.004$) after the CXL treatment. No statistically significant difference was found between the 0.25% G-CXL group and the UVA-CXL group ($p>0.05$).

IVCM scans:

Nerves—Seven days after the CXL treatment, nerve density diminished in all CXL groups (Table 1, $p < 0.001$), although it was statistically significantly severe in the UVA-CXL group compared to the 0.20% G-CXL and 0.25% G-CXL groups ($p < 0.05$). Fourteen days after the CXL treatment, no statistically significant difference in the nerve density was found among the 0.20% G-CXL group (Figure 2B), the 0.25% G-CXL group (Figure 2C), and the control group (Figure 2A), but the nerve density in the UVA-CXL group (Figure 2D) was statistically significant diminished compared to that in the control group (Table 1, $p < 0.05$).

Stroma—The IVCM scan results on day 7 and 14 were similar in all groups. Analysis of keratocyte density at different depths is shown in Table 2 and Table 3. Keratocyte nuclei in the subepithelial cells to the mid-stroma in the UVA-CXL group had disappeared or shrunk (Figure 2D,H,L). A hyperreflective needle-shaped structure was visible in the mid-stroma (Figure 2L). The morphology of the keratocytes remained normal in the posterior stroma (Figure 2P). In the 0.20% G-CXL group and the 0.25% G-CXL group, reduction in keratocytes was noticed in the subepithelial cells to the anterior stroma (Figure 2B,C,F,G). The remaining keratocytes were activated, showing gray, enlarged, star-shape plasma (Figure 2J, K). A needle-shaped structure was visible in the

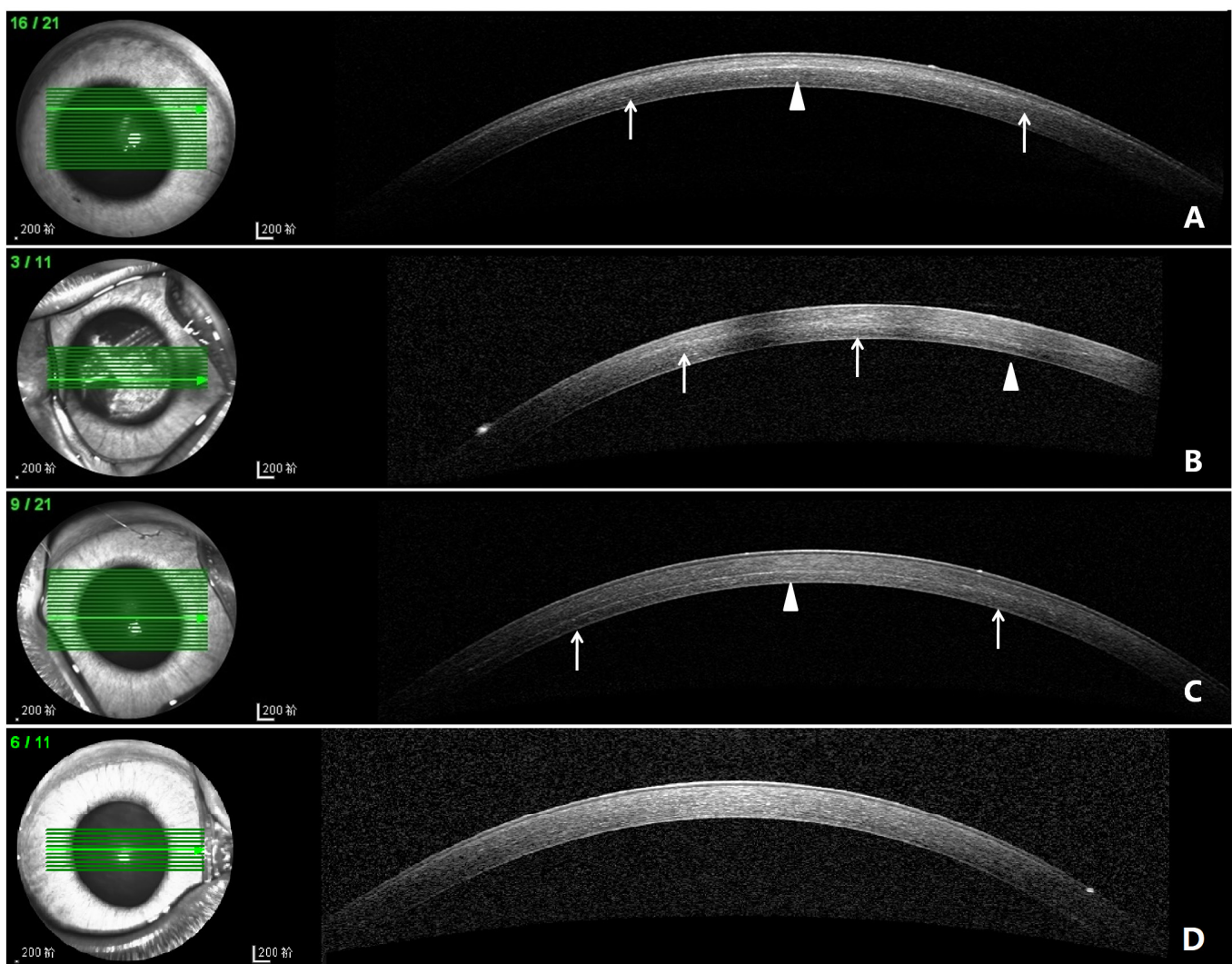


Figure 1. ASOCT images of each group on day 14. **A:** DL in 0.20% G-CXL group, located in the anterior stroma (arrows). The deepest position was on the superior edge of pupil (arrowhead). **B:** DL in 0.25% G-CXL group, located in anterior-mid stroma (arrows). The deepest position was on the nasal edge of pupil. **C:** DL in UVA-CXL group (arrows). The deepest position was in the cornea center (arrowheads). **D:** The control group, no DL was noticed.

TABLE 1. SUBEPITHELIAL NERVE DENSITY OF EACH GROUP AT DIFFERENT TIME POINT(MM/MM²).

| Duration | 0.20% G-CXL | 0.25% G-CXL | UVA-CXL | control | P |
|--|----------------------------|----------------------------|---------------------------|--------------|--------|
| 7-day observation (n=5 in each group) | | | | | |
| pre-CXL | 4710.5±506.8 | 4616.6±590.7 | 4644.6±250.1 | 4632.5±700.6 | 0.995 |
| post-CXL | 1988.0±667.1 ^{†‡} | 2089.6±397.7 ^{†‡} | 713.4±282.8 [†] | 4517.9±397.1 | <0.001 |
| 14-day observation (n=5 in each group) | | | | | |
| pre-CXL | 4594.0±367.0 | 4582.5±452.1 | 4594.8±159.3 | 4653.5±237.2 | 0.985 |
| post-CXL | 4446.2±357.2 ^{†‡} | 4500.4±230.5 ^{†‡} | 841.9±512.5 ^{†‡} | 4627.0±215.4 | <0.001 |

[†] p<0.05 compared to the control group, [‡] p<0.05 compared to the UVA-CXL group. N=5 in each group.

anterior stroma (Figure 2, F, G). The posterior stroma was normal (Figure 2N,O). In the control group, the keratocytes decreased in the subepithelial stroma (Figure 2A), while the rest of the stroma remained normal (Figure 2E,I,M).

Endothelial cells: In the 0.20% G-CXL group (Figure 2R) and the control group (Figure 2Q), no endothelial cell damage was observed on day 7 and 14 after the CXL treatment. Seven days after the 0.25% G-CXL treatment, endothelial cell border was blurred, and minimum cell damage was observed, which improved by day 14 after the CXL treatment (Figure 2S). Obvious endothelial damage was observed in the UVA-CXL group (Figure 2T).

No difference in the endothelial cell count among the four groups was found before treatment. Seven days after the CXL treatment, endothelial cell loss existed in all CXL groups (Table 4, p<0.001), and it was statistically significantly severe in the UVA-CXL group (41.9%) compared to the 0.20% G-CXL (19.4%) and 0.25% G-CXL groups (13.1%; p<0.05). Fourteen days after the CXL treatment, no statistically significant difference in endothelial cell loss was found among the 0.20% G-CXL group (11.7%), the 0.25% G-CXL group (6.8%), and the control group, while endothelial cell loss in the UVA-CXL group (31.8%) was statistically significant higher compared to that in the control group (Table 4, p<0.05).

Biomechanics measurements: Seven days after the CXL treatment, Young's modulus was 15.04±3.800 MPa in the 0.20% G-CXL group, 21.24±6.770 MPa in the 0.25% G-CXL group, 18.76±3.340 MPa in the UVA-CXL group, and 12.10±3.870 MPa in the control group. The stress at 10% strain was 0.73±0.17, 1.20±0.25, 1.01±0.30, and 0.71±0.28 MPa, respectively. A similar stiffening effect was observed on day 14 after the CXL treatment. Young's modulus in the 0.20% G-CXL group, the 0.25% G-CXL group, the UVA-CXL group, and the control group was 16.65±3.190, 19.12±2.390, 22.83±4.380, and 12.66±3.100 MPa and the stress at 10%

strain was 0.83±0.12, 0.97±0.04, 1.23±0.30, and 0.68±0.23 MPa, respectively.

On day 7 and 14 after CXL, the differences in Young's modulus and the stress at 10% strain among the four groups were statistically significant (p<0.05, Figure 3). Young's modulus and the stress at 10% strain in the 0.25% G-CXL group and the UVA-CXL group were statistically significantly increased in comparison with the control group (p<0.05, Figure 3). No statistically significant differences were found between the 0.25% G-CXL group and the UVA-CXL group (p>0.05, Figure 3).

Correlation of biomechanical properties and DL depth: As shown in Figure 4, with a higher concentration of genipin solution, a deeper DL and an increasing Young's modulus and stress at 10% strain were observed. The DL depth positively correlated with Young's modulus (r=0.467, p=0.014) and stress (r=0.413, p=0.032).

DISCUSSION

In this study, we chose 0.20% and 0.25% genipin solution for use on rabbit corneas. During the 14-day observation, changes in the corneal structure and biomechanical properties were evaluated in comparison with the UVA-CXL group, and the correlation was analyzed. Observation in this study showed a similar stiffening effect on the corneas between the 0.25% G-CXL and UVA-CXL groups at least for 14 days, while G-CXL was less toxic to nerves, keratocytes, and endothelium cells. In this study, topical corticosteroid was not used after the CXL treatment, to avoid possible interference with the corneal biomechanics [18].

This is the first study to reveal well-defined demarcation lines in a genipin crosslinked cornea with the help of ASOCT. In this and a previous study [19], the deepest part of the DL in the UVA/riboflavin crosslinked cornea was mainly located in the central cornea with a shallower course toward the periphery. However, in the G-CXL group, the deepest part was mainly located in the paracentral cornea. We presume the

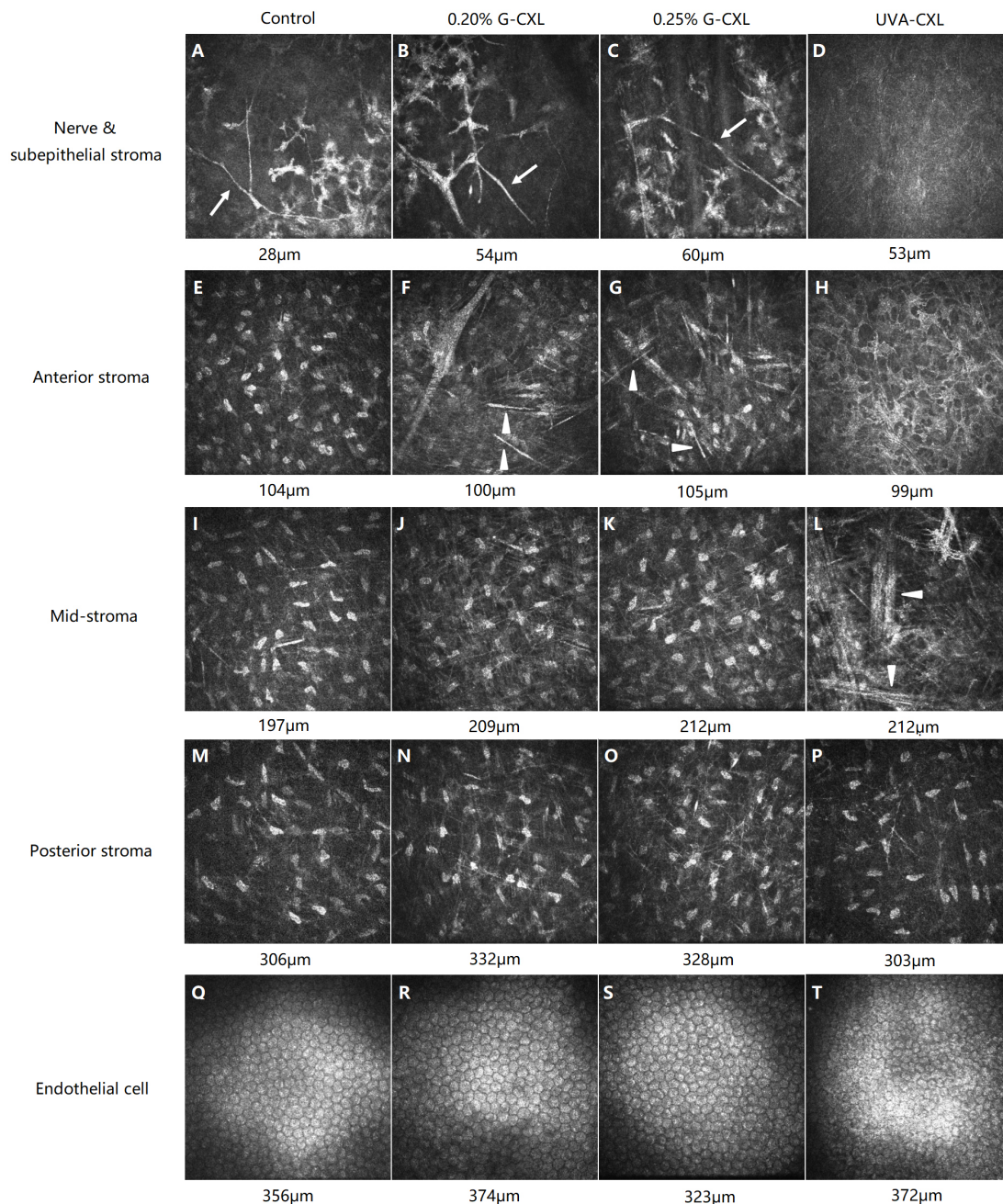


Figure 2. IVCN images of each group on day 14 after the CXL. The control group: nerves existed in subepithelium stroma (**A**, arrow) while keratocytes reduced (**A**). Keratocytes in deeper stroma (**E**, **I**, **M**) and endothelial cell (**Q**) remained normal. 0.20% G-CXL group: visible nerves (**B**, arrow) and reduced keratocytes (**B**, **F**) were noticed. Needle-shaped structure existed in anterior stroma (**F**, arrowhead). Keratocytes in anterior (**F**) and mid-stroma (**J**) were activated. Posterior stroma (**N**) and endothelial cell were normal (**R**). 0.25% G-CXL group: nerves were visible (**C**, arrow). Needle-shaped structure existed in anterior stroma (**G**, arrowhead). Keratocytes in anterior to mid-stroma were reduced and activated (**G**, **K**). Posterior stroma (**O**) and endothelial cell (**S**) was normal. UVA-CXL group: nerves (**D**) and most keratocytes in anterior to mid-stroma (**D**, **H**, **L**) disappeared. Needle-shaped structure existed in mid-stroma (**L**, arrowhead). Posterior stroma (**P**) was normal. Endothelial cell was obvious damaged (**T**).

TABLE 2. KERATOCYTES DENSITY AT DIFFERENT DEPTH OF STROMA 7 DAYS AFTER CXL (CELL/MM²).

| Duration | 0.20% G-CXL | 0.25% G-CXL | UVA-CXL | control | P |
|--|--------------|--------------|-------------|------------|--------|
| Subepithelial stroma at 50 µm depth | | | | | |
| pre CXL | 452.6±15.8 | 464.1±5.8 | 461.2±23.5 | 456.1±41.8 | 0.95 |
| post CXL | 245.9±76.1†‡ | 171.7±41.9†‡ | 78.7±54.7† | 308.7±39.2 | <0.001 |
| P | <0.001 | 0.001 | <0.001 | <0.001 | |
| Anterior stroma at 100 µm depth | | | | | |
| pre CXL | 364.8±11.6 | 359.5±12.0 | 367.9±14.2 | 359.2±22.1 | 0.831 |
| post CXL | 255.5±34.3†‡ | 244.2±16.3†‡ | 89.6±30.9† | 359.8±17.9 | <0.001 |
| P | 0.001 | 0.001 | <0.001 | 0.966 | |
| Mid-stroma ant 200 µm depth | | | | | |
| pre CXL | 308.5±10.3 | 298.6±3.6 | 299.3±9.1 | 312.9±9.2 | 0.087 |
| post CXL | 293.5±17.3‡ | 295.5±3.8‡ | 197.5±52.5† | 317.2±7.0 | <0.001 |
| P | 0.187 | 0.523 | 0.003 | 0.438 | |
| Posterior stroma at 300 µm depth | | | | | |
| pre CXL | 261.5±12.5 | 263.2±19.2 | 264.1±15.1 | 258.2±14.2 | 0.934 |
| post CXL | 272.1±16.3 | 268.4±20.7 | 246.6±17.7 | 259.4±19.7 | 0.242 |
| P | 0.322 | 0.762 | 0.154 | 0.917 | |

† p<0.05 compared to the control group, ‡ p<0.05 compared to the UVA-CXL group. N=5 in each group.

difference results from the surgical method. In the present study, genipin solution was applied on the central cornea, but not limited to the cornea. Thus, genipin solution spread over the conjunctiva sac, and the paracentral cornea may have been soaked in the genipin solution, which could have led to

better penetration. Avila et al. [20] reported the usage of a vacuum device in G-CXL surgery to ensure genipin affected the central cornea only. In the future, a similar device should be considered in G-CXL surgery for better permeability,

TABLE 3. KERATOCYTES DENSITY AT DIFFERENT DEPTH OF STROMA 14 DAYS AFTER CXL(CELL/MM²).

| Duration | 0.20% G-CXL | 0.25% G-CXL | UVA-CXL | control | P |
|--|-------------|-------------|-------------|-------------|--------|
| Subepithelial stroma at 50 µm depth | | | | | |
| pre CXL | 450.0±35.8 | 457.7±33.4 | 459.2±38.0 | 452.9±30.2 | 0.977 |
| post CXL | 286.2±25.3‡ | 193.8±62.5‡ | 77.3±77.7† | 279.7±50.9 | 0.001 |
| P | <0.001 | 0.003 | <0.001 | <0.001 | |
| Anterior stroma at 100 µm depth | | | | | |
| pre CXL | 361.3±10.5 | 355.3±10.1 | 363.1±23.2 | 358.7±17.4 | 0.95 |
| post CXL | 356.6±17.1‡ | 338.9±28.5‡ | 112.5±83.5† | 353.9±14.4 | <0.001 |
| P | 0.716 | 0.4 | 0.001 | 0.644 | |
| Mid-stroma ant 200 µm depth | | | | | |
| pre CXL | 318.5±14.7 | 307.9±8.1 | 312.1±25.2 | 308.8±14.8 | 0.785 |
| post CXL | 302.3±17.2‡ | 306.0±40.1‡ | 228.8±31.2† | 3104.2±11.2 | 0.002 |
| P | 0.171 | 0.938 | 0.006 | 0.592 | |
| Posterior stroma at 300 µm depth | | | | | |
| pre CXL | 265.0±23.6 | 265.2±14.2 | 267.0±22.5 | 257.3±20.0 | 0.901 |
| post CXL | 270.2±6.2 | 268.6±12.6 | 262.1±32.0 | 259.5±19.4 | 0.854 |
| P | 0.695 | 0.772 | 0.812 | 0.86 | |

† p<0.05 compared to the control group, ‡ p<0.05 compared to the UVA-CXL group. N=5 in each group

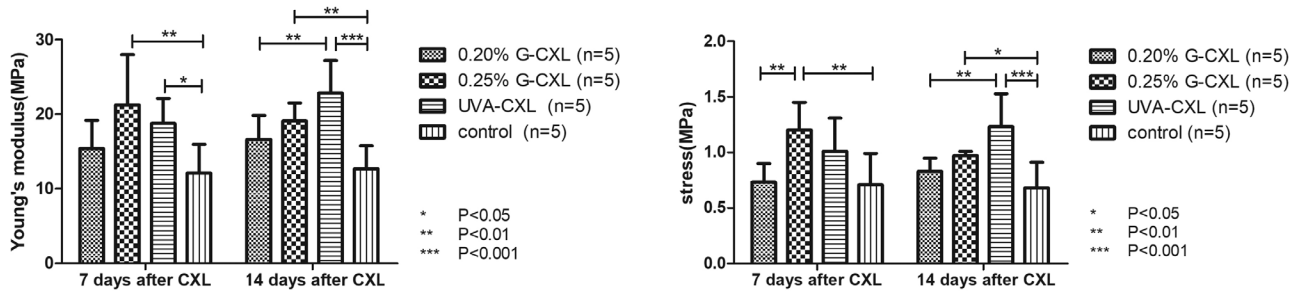


Figure 3. Young’s modulus and stress at 10% strain of treated and control eyes.

and avoidance of non-specific cross-linking effects of surrounding structures.

Ex vivo studies showed genipin can increase the cornea Young’s modulus and stress in a concentration-dependent

manner [10]. In the present study, the tensile stress test showed that the cornea strength increased in the order of the control group, the 0.20% G-CXL group, and the 0.25% G-CXL group on day 7 and 14 after CXL treatment. This result indicated

TABLE 4. ENDOTHELIAL CELL DENSITY OF EACH GROUP AT DIFFERENT TIME POINT(CELL/MM²).

| Duration | 0.20% G-CXL | 0.25% G-CXL | UVA-CXL | control | P |
|--|----------------------------|---------------------------|---------------------------|--------------|--------|
| 7-day observation (n=5 in each group) | | | | | |
| pre-CXL | 2471.6±216.3 | 2304.9±204.1 | 2353.0±194.4 | 2504.4±139.6 | 0.425 |
| post-CXL | 1991.6±381.1 ^{†‡} | 2003.7±188.0 [‡] | 1367.0±308.1 [†] | 2491.0±134.5 | <0.001 |
| change% | -19.4% | -13.1% | -41.9% | -0.5% | |
| 14-day observation (n=5 in each group) | | | | | |
| pre-CXL | 2426.1±208.2 | 2424.9±58.0 | 2555.3±256.9 | 2542.2±106.3 | 0.595 |
| post-CXL | 2141.7±554.3 | 2260.9±93.5 | 1716.3±225.7 [†] | 2493.0±117.5 | 0.03 |
| change% | -11.7% | -6.8% | -32.8% | -2.0% | |

[†] p<0.05 compared to the control group, [‡] p<0.05 compared to the UVA-CXL group. N=5 in each group

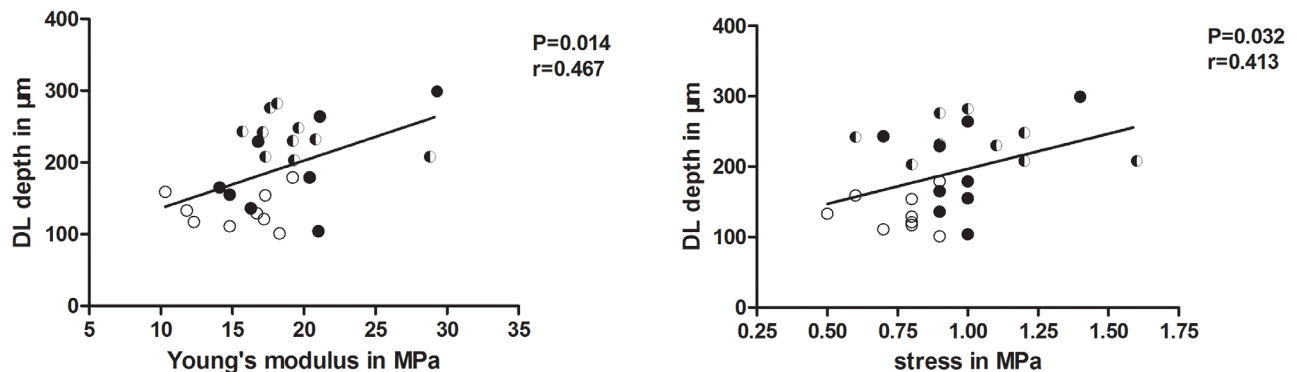


Figure 4. Correlations of depth of demarcation line and Young’s modulus (left) stress (right) at 10% strain(n=27) circle ○, 0.20% G-CXL; dot ●, 0.25%G-CXL; half filled circleUVA-CXL.

that dose dependence and the stiffness effect of G-CXL last at least 14 days. Although a decrease in Young's modulus and stress was observed in the 0.25% G-CXL group over 14 days after the CXL treatment, the 0.25% G-CXL group still showed a similar biomechanical effect as the UVA-CXL group. To clarify the stability of the G-CXL biomechanical effect and the formation of a DL, long-term observation is needed in the future.

The demarcation line is considered the transition zone between the crosslinked and untreated corneal stroma. Thus, the DL can be used as a measure of the extension of CXL treatment into the stroma [21,22]. Although in vivo corneal biomechanical measurements are available in the clinical setting, the test results of such techniques are controversial [23]. The correlation analysis in the present study showed that the DL depth positively correlated with Young's modulus and stress. Thus, the DL may be a helpful measure of the corneal stiffness. However, more research is needed.

The IVCN scan showed a reduction in the keratocytes in the anterior stroma in the control group, which indicated epithelial debridement may cause keratocyte loss [5]. However, the keratocyte cell counts, nerve density, and endothelial cell density in all CXL groups decreased after the CXL treatment, when compared to the control group, but the decreases were more obvious in the UVA-CXL group. Song et al. [24] reported minimum endothelial damage of 0.20% G-CXL on day 1 after the CXL treatment compared with UVA-CXL. In the present study, the endothelial cell count decreased in the G-CXL group on day 14 after the CXL treatment (the 0.20% G-CXL group, 11.7%, versus the 0.25% G-CXL group, 6.8%). The decrease is within the range of endothelial cell loss after cataract surgery (4–25%) [25], while in the UVA-CXL group, the endothelial cell loss was 32.8%. Considering the thickness of the rabbit corneas is thinner, we presumed that genipin may be a safer CXL procedure in patients with thin corneas.

Moreover, IVCN detected a hyper-refractive needle-shaped structure in the corneal stroma after CXL treatment. Haze or scarring sometimes can be observed after CXL treatment or epithelial debridement, which is usually presented as hyper-reflective extracellular tissue surrounding keratocyte nuclei or hyper-reflective tissue without cells on IVCN [26]. Thus, the needle-shaped structure is different from haze or scarring. Mazzotta et al. reported similar needle-shaped structure changes in UVA/riboflavin crosslinked patients [27]. The authors hypothesized that the needle-shaped structure represented newly replaced collagen fiber and new connections formed between lamellas. In the present study, the needle-shaped structure existed in the stroma near the DL

(anterior to the mid-stroma in the G-CXL group and mid to the posterior stroma in the UVA-CXL group). As mentioned above, the DL is considered a transition zone between the crosslinked and untreated corneal stroma. These findings support the hypothesis of the Mazzotta team. However, more studies that explore the theory of the formation of such a structure are needed.

There are limitations in the present study. First, the surgical method of G-CXL needs improvement. Devices that ensure genipin affects only the central cornea should be considered. Second, control groups with sham treatment should be set in a future study. Moreover, a longer observation period of biomechanical properties and the safety of G-CXL is needed.

Conclusion: The concentration of 0.25% genipin enhances corneal biomechanical properties as long as 14 days after CXL treatment. The concentrations of 0.20% and 0.25% genipin are less cytotoxic to the corneal nerves, keratocytes, and endothelial cells compared to UVA-CXL. A demarcation line is formed after G-CXL treatment, and the depth is positively related to the biomechanical properties.

ACKNOWLEDGMENTS

The authors thank Professor Fan Song and Dr. Ruiqi Du from the state key laboratory of nonlinear mechanics in China for the help in the tensile stain test. The study was financially supported by the National Natural Science Foundation of China(11372011), Beijing Natural Science Foundation(7142159) and Beijing Natural Science Foundation (7192210).

REFERENCES

1. Sedaghat M, Naderi M, Zarei-Ghanavati M. Biomechanical parameters of the cornea after collagen crosslinking measured by waveform analysis. *J Cataract Refract Surg* 2010; 36:1728-31. [PMID: 20870120].
2. Grewal DS, Brar GS, Jain R, Sood V, Singla M, Grewal SP. Corneal collagen crosslinking using riboflavin and ultraviolet-A light for keratoconus: one-year analysis using Scheimpflug imaging. *J Cataract Refract Surg* 2009; 35:425-32. [PMID: 19251133].
3. Dahl BJ, Spotts E, Truong JQ. Corneal collagen cross-linking: an introduction and literature review. *Optometry* 2012; 83:33-42. [PMID: 22153823].
4. Raiskup-Wolf F, Hoyer A, Spoerl E, Pillunat LE. Collagen crosslinking with riboflavin and ultraviolet-A light in keratoconus: long-term results. *J Cataract Refract Surg* 2008; 34:796-801. [PMID: 18471635].

5. Wollensak G, Spoerl E, Wilsch M, Seiler T. Keratocyte apoptosis after corneal collagen crosslinking using riboflavin/UVA treatment. *Cornea* 2004; 23:43-9. [PMID: 14701957].
6. Wasilewski D, Mello G, Moreira H. Impact of Collagen Cross-linking on Corneal Sensitivity in Keratoconus Patients. *Cornea* 2013; 32:899-902. [PMID: 23263221].
7. Wollensak G, Sporl E, Reber F, Pillunat L, Funk R. Corneal Endothelial Cytotoxicity of Riboflavin/UVA Treatment in vitro. *Ophthalmic Res* 2003; 35:324-8. [PMID: 14688422].
8. Cagil N, Sarac O, Can GD, Akcay E, Can ME. Outcomes of corneal collagen crosslinking using a customized epithelial debridement technique in keratoconic eyes with thin corneas. *Int Ophthalmol* 2017; 37:103-9. [PMID: 27097560].
9. Avila MY, Gerena V, Navia J. Corneal crosslinking with genipin, comparison with UV-Riboflavin in ex-vivo model. *Mol Vis* 2012; 18:1068-73. [PMID: 22605919].
10. Avila MY, Navia JL. Effect of genipin collagen crosslinking on porcine corneas. *J Cataract Refract Surg* 2010; 36:659-64. [PMID: 20362860].
11. Wang M, Corpuz CC. Effects of scleral cross-linking using genipin on the process of form-deprivation myopia in the guinea pig: a randomized controlled experimental study. *BMC Ophthalmol* 2015; 15:89-[PMID: 26220299].
12. Liu Z, Zhou Q, Zhu J, Xiao J, Wan P, Zhou C, Huang Z, Qiang N, Zhang W, Wu Z, Quan D, Wang Z. Using genipin-cross-linked acellular porcine corneal stroma for cosmetic corneal lens implants. *Biomaterials* 2012; 33:7336-46. [PMID: 22795849].
13. Lai JY. Biocompatibility of genipin and glutaraldehyde cross-linked chitosan materials in the anterior chamber of the eye. *Int J Mol Sci* 2012; 13:10970-85. [PMID: 23109832].
14. Grolnik M, Szczubialka K, Wowra B, Dobrowolski D, Orzechowska-Wylegala B, Wylegala E, Nowakowska M. Hydrogel membranes based on genipin-cross-linked chitosan blends for corneal epithelium tissue engineering. *J Mater Sci Mater Med* 2012; 23:1991-2000. [PMID: 22569736].
15. Wollensak G, Spoerl E, Seiler T. Riboflavin/ultraviolet-A-induced collagen crosslinking for the treatment of keratoconus. *Am J Ophthalmol* 2003; 135:620-7. [PMID: 12719068].
16. Aggarwal S, Cavalcanti BM, Regali L, Cruzat A, Trinidad M, Williams C, Jurkunas UV, Hamrah P. In Vivo Confocal Microscopy Shows Alterations in Nerve Density and Dendritiform Cell Density in Fuchs' Endothelial Corneal Dystrophy. *Am J Ophthalmol* 2018; 196:136-44. [PMID: 30194928].
17. Meijering E, Jacob M, Sarria JC, Steiner P, Hirling H, Unser M. Design and validation of a tool for neurite tracing and analysis in fluorescence microscopy images. *Cytometry A* 2004; 58:167-76. [PMID: 15057970].
18. Spoerl E, Zubaty V, Terai N, Pillunat LE, Raiskup F. Influence of high-dose cortisol on the biomechanics of incubated porcine corneal strips. *J Refract Surg* 2009; 25:S794-8. [PMID: 19772253].
19. Koller T, Schumacher S, Fankhauser F 2nd, Seiler T. Riboflavin/Ultraviolet A Crosslinking of the Paracentral Cornea. *Cornea* 2013; 32:165-8. [PMID: 23187160].
20. Avila MY, Narvaez M, Castaneda JP. Effects of genipin corneal crosslinking in rabbit corneas. *J Cataract Refract Surg* 2016; 42:1073-7. [PMID: 27492108].
21. Khandelwal SS, Randleman JB. Current and future applications of corneal cross-linking. *Curr Opin Ophthalmol* 2015; 26:206-13. [PMID: 25784110].
22. Moramarco A, Iovieno A, Sartori A, Fontana L. Corneal stromal demarcation line after accelerated crosslinking using continuous and pulsed light. *J Cataract Refract Surg* 2015; 41:2546-51. [PMID: 26703505].
23. Bak-Nielsen S, Pedersen IB, Ivarsen A, Hjortdal J. Dynamic Scheimpflug-based assessment of keratoconus and the effects of corneal cross-linking. *J Refract Surg* 2014; 30:408-14. [PMID: 24972407].
24. Song W, Tang Y, Qiao J, Li H, Rong B, Yang S, Wu Y, Yan X. The comparative safety of genipin versus UVA-riboflavin crosslinking of rabbit corneas. *Mol Vis* 2017; 23:504-13. [PMID: 28761323].
25. Ho JW, Afshari NA. Advances in cataract surgery: preserving the corneal endothelium. *Curr Opin Ophthalmol* 2015; 26:22-7. [PMID: 25415300].
26. Mazzotta C, Hafezi F, Kymionis G, Caragiuli S, Jacob S, Traversi C, Barabino S, Randleman JB. In Vivo Confocal Microscopy after Corneal Collagen Crosslinking. *Ocul Surf* 2015; 13:298-314. [PMID: 26142059].
27. Mazzotta C1, Traversi C, Baiocchi S, Caporossi O, Bovone C, Sparano MC, Balestrazzi A, Caporossi A. Corneal healing after riboflavin ultraviolet-A collagen cross-linking determined by confocal laser scanning microscopy in vivo: early and late modifications. *Am J Ophthalmol* 2008; 146:527-33. [PMID: 18672225].

Articles are provided courtesy of Emory University and the Zhongshan Ophthalmic Center, Sun Yat-sen University, P.R. China. The print version of this article was created on 6 October 2019. This reflects all typographical corrections and errata to the article through that date. Details of any changes may be found in the online version of the article.